Chinese Chemical Letters 33 (2022) 2726–2730

Contents lists available at ScienceDirect

Chinese Chemical Letters

journal homepage: www.elsevier.com/locate/cclet

Synergistic catalytic ozonation of toluene with manganese and cerium varies at low temperature

Qi Gan[a], Mingli Fu[a,b,c,d,*], Peng Liu[a], Yuchen Zhang[a], Juxia Xiong[a], Jinping Zhong[a], Lei Liu[a], Junliang Wu[a,b,c,d], Xiaojun Niu[a], Yun Hu[a], Daiqi Ye[a,b,c,d]

[a] School of Environment and Energy, South China University of Technology, Guangzhou 510006, China
[b] National Engineering Laboratory for VOCs Pollution Control Technology and Equipment (SCUT), Guangzhou 510006, China
[c] Guangdong Provincial Key Laboratory of Atmospheric Environment and Pollution Control (SCUT), Guangzhou 510006, China
[d] Guangdong Provincial Engineering and Technology Research Center for Environmental Risk Prevention and Emergency Disposal (SCUT), Guangzhou 510006, China

ARTICLE INFO

Article history:
Received 9 July 2021
Revised 20 August 2021
Accepted 2 September 2021
Available online 9 September 2021

Keywords:
Ozone
Oxygen vacancy
Active oxygen species
Synergism
Pathway

ABSTRACT

The temperature of waste gas in refuse transfer station, airport smoking area, and RTO terminal is low, which needs deep oxidation. Catalytic ozonation is one of the most effective treatment techniques in these scenarios. In this study, we reported that catalysts were modified under the condition of magnetic field to simulate the low temperature dynamic conditions of low concentration toluene for catalytic ozonation. This paper aims to explore the relationship between oxygen vacancy and active oxygen species, and the specific pathways of toluene oxidation. The study found that citric acid can enhance the synergistic effect between Mn and Ce, and promote the generation of oxygen vacancies. The surface molecule adsorption oxygen is more conducive to catalytic oxidation than subsurface atom adsorption oxygen. Finally, we proposed the main pathways of toluene in this reaction system, which runs through the whole process of the reaction.

Volatile organic compounds (VOCs) are important precursors of many atmospheric environmental problems. Among many air pollution treatment methods, regenerative thermal oxidizer (RTO) and regenerative catalytic oxidation (RCO) are widely used. Both of them have high purification efficiency. Among them, RCO has high cost, selectivity to pollutant types and small concentration range of waste gas treatment [1]. RTO has low cost and wide application range of waste gas concentration, and can treat a variety of organic waste gases [2]. After many considerations, the industry of pharmacy, printing, coating, paint coating [3] line and so on usually adopts RTO method to deal with the exhaust gas. With the change of external environment and the strictness of relevant standards, some of the tail gas after RTO treatment cannot meet the emission standard. At this time, the exhaust gas temperature is in the range of 0–90 °C [4], which has the characteristics of low concentration, low temperature and constant fluctuation of temperature range. Therefore, in order to solve this problem, this study simulated the catalytic oxidation of low concentration toluene under low temperature dynamic conditions of 30–130 °C.

There are many methods to remove VOCs at low temperature. Among them, photocatalysis, low temperature plasma and catalytic ozonation are widely used. Photocatalysis is more sensitive to light and requires higher light conditions. Low temperature plasma method requires high discharge and high energy consumption. Considering the complexity and economy of practical industrial application, catalytic ozonation method magnifies its advantages. Due to the strong oxidation of ozone, VOCs can be removed efficiently under mild conditions. In addition, when the catalyst and ozone cooperate to remove VOCs, ozone can also be decomposed, so as to achieve the purpose of simultaneously complete purification of VOCs and O_3 [5–7]. However, in previous studies, the mineralization rate of VOCs is generally low, the service life is short, especially the CO_2 selectivity is low. If we want to improve the mineralization rate of VOCs, we need to increase the reaction temperature, which is difficult to fully reflect the strong oxidation advantage of O_3. Even under such conditions, CO_2 selectivity is still very low. Therefore, this study aims to solve the mentioned-above problems in the field of catalytic ozonation of VOCs.

* Corresponding author at: School of Environment and Energy, South China University of Technology, Guangzhou, China.
E-mail address: mlfu@scut.edu.cn (M. Fu).

https://doi.org/10.1016/j.cclet.2021.09.006
1001-8417/

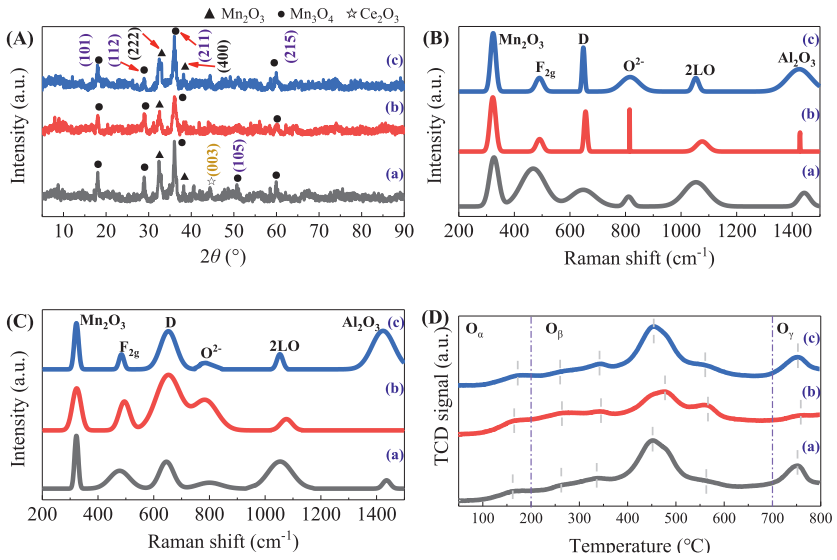

Fig. 1. (A) XRD images; (B) UV-Raman-fresh; (C) UV-Raman-used; (D) H_2-TPR. (a) MnCe/Al_2O_3; (b) MnCe/Al_2O_3-CA; (c) MnCe/Al_2O_3-PEG.

In the field of catalytic oxidation, Al_2O_3 is widely used as the carrier of catalyst because of its low price, large specific surface area and mechanical strength [8,9]. For active components, studies have shown that manganese based catalysts have advantages in catalytic ozonation of VOCs [10–12], especially in the decomposition ability of ozone [13–15]. In the catalytic ozonation of VOCs, it is necessary for the catalyst to have strong ozone decomposition performance [16]. The active oxygen species [17–20] decomposed by Mn can promote the decomposition of VOCs, so as to achieve the purpose of VOCs abatement [21–23].

Catalytic ozonation of VOCs requires not only higher oxidation rate of VOCs, but also higher mineralization rate. The addition of Mn can effectively improve the decomposition rate of toluene, but its contribution to the mineralization rate of toluene is not ideal. The rare earth element Ce has strong electron transfer ability because of its more d and f empty orbitals, which is conducive to the generation of oxygen vacancies [24,25]. Studies have shown that rich oxygen vacancies are conducive to the decomposition and mineralization of VOCs [26]. Therefore, the addition of rare earth element Ce can effectively improve the mineralization rate of toluene.

The results show that active oxygen species and oxygen vacancy are beneficial to improve the decomposition rate and mineralization rate of VOCs. However, the species of reactive oxygen species and their relationship with oxygen vacancies have not been studied thoroughly. Therefore, we prepare the modified and unmodified MnCe/Al_2O_3 under the condition of magnetic field by using the effect of electrostatic adsorption. The three properties (activity, selectivity and stability) of the catalyst were evaluated under simulated conditions. The catalysts were characterized by XRD, SEM, TEM, EDS, BET, XPS, Raman, H_2-TPR, O_2-TPD, FTIR and TA-MS to explore the synergistic effect between Mn and Ce. In addition, the relationship among oxygen vacancy, active oxygen species and catalyst properties was studied. The decomposition pathway of toluene in this reaction system was further specified.

XRD characterization can qualitatively study the structure of the catalyst. Fig. 1A shows the XRD patterns of MnCe/Al_2O_3, MnCe/Al_2O_3-CA and MnCe/Al_2O_3-PEG. The XRD peaks at 2θ of 19.1°, 28.9°, 36.2°, 50.9° and 60.1° are attributed to the (101), (112), (211), (105) and (215) planes [27,28] of Mn_3O_4 respectively, which are consistent with the standard card (JCPDS No. 24–0734). The XRD peaks at 2θ of 32.5° and 38.2° belong to (222) and (400) planes of Mn_2O_3, respectively [29]. The XRD peak at 2θ of 44.4° belongs to the (003) plane of Ce_2O_3 (JCPDS No. 89–8434). Three catalysts mainly show the characteristic structure of Mn_2O_3 and Mn_3O_4, and their peak intensity are generally relatively decrease. Their characteristic peaks of Al_2O_3 and CeO_x are no obvious. It shows that MnO_x and CeO_x are distributed uniformly on Al_2O_3 surface [30]. This is consistent with the EDS results (Fig. S1 in Supporting information). The peak of MnCe/Al_2O_3 is narrow, indicating that the crystal particles of MnCe/Al_2O_3 are relatively large, and the specific surface area is the smallest, which is consistent with the BET results (Fig. S2 in Supporting information). The peaks of MnCe/Al_2O_3-CA are broad and not obvious, while those of MnCe/Al_2O_3 are sharp and obvious, indicating that the modifier destroys the crystal structure of the catalyst. The results should be assigned to the destruction of citric acid makes the crystallinity of MnCe/Al_2O_3-CA is lower and the lattice fringes are not shown in TEM (Fig. S3 in Supporting information), which indicates that the lattice pattern is more amorphous. Amorphous can help to expose more defect sites, which indicates that the modified catalyst can produce more defect sites and expand the active area of the catalyst surface [31].

In order to detect the structure of the catalysts, UV Raman was characterized shown in Fig. 1B. The diffraction peaks at 325 cm^{-1}, 465 cm^{-1}, 815 cm^{-1}, 1065 cm^{-1} and 1430 cm^{-1} belong to the peaks of the Mn_2O_3, F_{2g} type fluorite structure of CeO_2, O^{2-}, second order longitudinal photon vibration 2LO of CeO_2 and Al_2O_3, respectively [32–35]. The Mn_2O_3 and O^{2-} of MnCe/Al_2O_3-CA and MnCe/Al_2O_3-PEG are red shifted. The results show that citric acid and polyethylene glycol affect the crystal structure of the support [36], leading to the formation of highly defect structure [37], and promoting the generation of oxygen vacancies. This is consistent with the SEM image of the catalyst (Fig. S1). The diffraction peak at 650 cm^{-1} belongs to the vibration peak of oxygen defect site species [38], which is caused by the synergistic effect of Mn and Ce [39]. The relative oxygen vacancy concentration of the catalyst can be expressed by the peak area ratio A_D/A_{F2g} at 650 cm^{-1} and 465 cm^{-1} [40]. The results showed that the oxygen vacancy concentration of the three catalysts followed the order of MnCe/Al_2O_3-CA (0.67) > MnCe/Al_2O_3-PEG (0.63) > MnCe/Al_2O_3 (0.61). Comparing the oxygen vacancy concentration measured by XPS and UV-Raman (denoted by $(O_b + O_c)/(O_a + O_b + O_c)$ and A_D/A_{F2g}, respectively), it was found that the oxygen vacancy concentrations of

the three catalysts were consistent. The oxygen vacancy caused by Ce is determined by XPS, while the total oxygen vacancy concentration of the catalyst was determined by UV-Raman. The results show that the total oxygen vacancy of the catalyst is caused by the interaction of Mn and Ce. Mn plays an important role in it.

The catalyst used for several times and recycled was characterized by UV-Raman, as shown in Fig. 1C. It can be seen from the figure that there is no obvious change in the peaks of Mn_2O_3. The F_{2g} peak of MnCe/Al_2O_3-CA and MnCe/Al_2O_3-PEG did not change obviously, but the F_{2g} peak of MnCe/Al_2O_3 changed obviously. The results show that MnCe/Al_2O_3-CA and MnCe/Al_2O_3-PEG exist stably before and after the reaction, while the structure of the catalyst MnCe/Al_2O_3 changes greatly after several cycles. Compared with the fresh catalyst, the peak area of oxygen defect site D of the three catalysts increased significantly. It shows that a large amount of oxygen in the catalyst escapes to form oxygen vacancies and participates in the reaction.

In order to investigate the reducibility of the catalyst and the mobility of oxygen on its surface, the H_2-TPR is shown in Fig. 1D. The peak below 250 °C is formed by the synergistic effect between MnO_x and CeO_x, which promotes the reduction of oxygen adsorption on the surface of oxygen vacancy [41]. The peak appeared at about 300 °C is formed by the transformation of MnO_2 to Mn_2O_3 [42,43]. The reduction peak of 420–460 °C is attributed to the transformation from Mn_2O_3 to Mn_3O_4 [44]. The reduction peak at about 500 °C is attributed to the transformation of Mn_3O_4 to MnO [45,46]. Among them, the area I is lower than 300 °C, which is attributed to the reduction of surface oxygen (SO) of the catalyst; the area II is from 300 °C to 500 °C, which is attributed to the reduction of subsurface oxygen (SSO) of the catalyst; the region III higher than 500 °C is attributed to the reduction bulk oxygen (BO) of the catalyst [47]. The relative content of different oxygen species is calculated as shown in Table S2 (Supporting information). The SO of MnCe/Al_2O_3-CA was significantly higher than the other two. The total relative content of SO and SSO of the three catalysts was higher. The results show that the addition of modifier changes the structure of catalyst carrier, promotes the synergistic effect of manganese oxide and cerium oxide, and improves the mobility of oxygen on the catalyst surface. Among them, citric acid has the greatest contribution to oxygen mobility. The addition of citric acid improves the CO_2 selectivity and mineralization rate of the catalyst, and improves the stability of CO_2 production.

The removal rate of toluene is shown in Fig. S7 (Supporting information). In order to prove the role of O_3 in the reaction, the activity of MnCe/Al_2O_3, MnCe/Al_2O_3-CA and MnCe/Al_2O_3-PEG catalysts were evaluated in the presence and absence of O_3, as shown in Fig. S7A. In the absence of O_3, the removal rates of toluene by the three catalysts were all close to 0, indicating that O_3 played a very important role in this study. In Figs. S7B-D are the multiple catalytic ozonation cycle reactions of the three catalysts. It can be seen from the figure that the five cycle reaction curves of MnCe/Al_2O_3 deviate from each other slightly, followed by MnCe/Al_2O_3-CA. The results show that MnCe/Al_2O_3 has better stability in toluene removal, and MnCe/Al_2O_3-CA takes the second place. Fig. S8 (Supporting information) shows the CO_x productivity of the three catalysts, in which Figs. S8A, C and E correspond to the CO_2 selectivity of the three catalysts respectively, and Figs. S8B, D and F correspond to the mineralization rate of the three catalysts respectively. It can be seen from Figs. S8A, C and E that in the five cycle reactions, MnCe/Al_2O_3-CA has relatively high CO_2 selectivity, while MnCe/Al_2O_3 has relatively high CO_2 stability. It can be seen from Fig. S8B, D and F that the mineralization rates of the three catalysts are similar in the five cycles. However, in the later stage of the reaction, the mineralization rate of MnCe/Al_2O_3-CA MnCe/Al_2O_3-CA is relatively high, and the stability of CO_x production is relatively strong.

With the repeated cycles of the reaction, the three properties of the catalyst all decreased to a certain extent. Combined with the analysis of UV-Raman characterization before and after the reaction, it may be due to the excessive oxygen vacancies in the catalyst, resulting in the serious change of charge distribution [48], resulting in the deformation and collapse of the catalyst framework structure. At the same time, the addition of modifier can promote the generation of oxygen vacancies and maintain the concentration of oxygen vacancies. The addition of citric acid enhanced the surface acidity and specific surface area of the catalyst to a certain extent. The increase of appropriate surface acidity did not destroy the catalyst structure due to the expansion of specific surface area. Therefore, citric acid has better contribution to the maintenance of catalyst structure and generation of oxygen vacancy. Through the comprehensive analysis of toluene removal rate and CO_x productivity, it is found that MnCe/Al_2O_3-CA has the best performance.

In order to further study the specific changes of catalysts in the reaction process, the three catalysts were characterized by *in-situ* Raman spectroscopy, as shown in Fig. 2. In O_2 atmosphere: from the initial stage of the reaction (*i.e.*, heating from 30 °C) to the middle stage of the reaction (130 °C), the D peak gradually becomes not obvious. The results showed that the relative oxygen vacancy concentration of the three catalysts decreased gradually. From the middle stage of reaction (130 °C) to the end stage of reaction (*i.e.*, cooling to 30 °C), the D peak gradually became obvious. The results showed that the relative oxygen vacancy concentration of the three catalysts increased gradually. It also shows that the oxygen vacancy is recovered and basically returned to the initial state of reaction. It is proved that the relative oxygen vacancy concentration of the catalyst is restored to the surface before the reaction, and the catalyst in this study has good stability and can be recycled for many times. The changes of the three catalysts in O_3 atmosphere are basically consistent with those in O_2 atmosphere. However, in O_3 atmosphere, the D peak of MnCe/Al_2O_3 and MnCe/Al_2O_3-PEG gradually becomes not obvious from the initial stage to the end of the reaction, which is slower than that of MnCe/Al_2O_3-CA. And the relative oxygen vacancy concentration of MnCe/Al_2O_3-CA recovered from the initial stage to the end of the reaction. The results show that MnCe/Al_2O_3-CA can produce living oxygen species more quickly and the ability of oxygen vacancy recovery is relatively strong. The strong oxygen vacancy recovery ability makes the catalyst reusable and has more practical value.

In order to explore the synergistic relationship between various influencing factors, T_{90} and its characteristic results were comprehensively analyzed, as shown in Figs. 3A–D. The T_{90} of the three catalysts in Fig. 3A is almost the same. With the increase of cycle reaction times, the T90 of citric acid tends to be stable, indicating that it can help to improve the stability of the catalyst. [D] and [Ce] represent the relative oxygen vacancy concentration formed by the synergistic action of Mn and Ce and the action of Ce in Fig. 3B. The [D]/[Ce] of MnCe/Al_2O_3 is less than 1, while the other two are more than 1. It show that the modifier is beneficial to the synergistic production of more oxygen vacancies by Mn and Ce. [Ce]/[Mn] of three catalysts are basically the same, while [Ce]/[O] and [D]/[O] have the opposite trend. It shows that the effect of modifier on the behavior of Mn is stronger than that of Ce. The ratio of [D] to [Mn], [O] and [Ce] all followe the order of MnCe/Al_2O_3-CA > MnCe/Al_2O_3-PEG > MnCe/Al_2O_3. The results show that modifier can enhance the synergistic effect between Mn and Ce. In Figs. 3C and D, the change trend of oxygen vacancy and active oxygen species density is basically the same. The higher the density of oxygen vacancy and surface active oxygen species, the better the performance of the catalyst.

In Tables S2 and S3 (Supporting information), the corresponding values of SO:SSO:BO and O_α:O_β:O_γ of three catalysts are basically the same, which indicates that the surface atom adsorbed oxy-

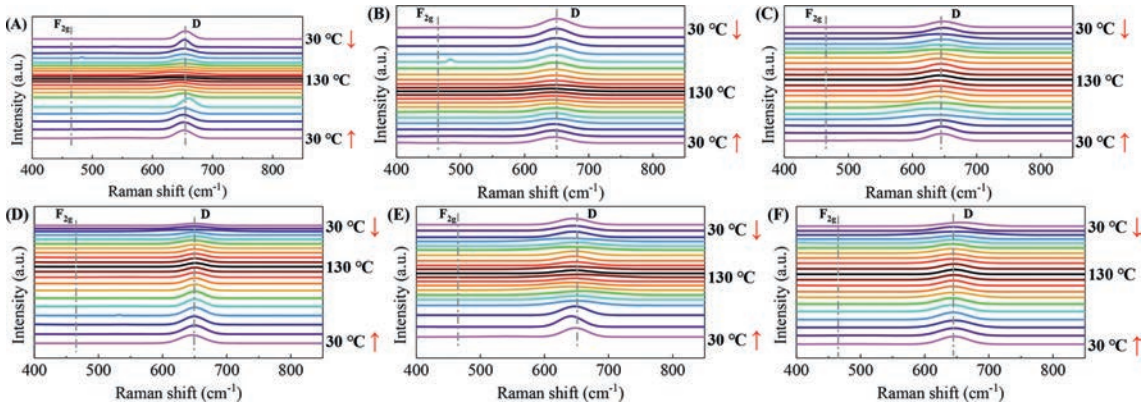

Fig. 2. O_2: (A) MnCe/Al_2O_3; (B) MnCe/Al_2O_3-CA; (C) MnCe/Al_2O_3-PEG. O_3: (D) MnCe/Al_2O_3; (E) MnCe/Al_2O_3-CA; (F) MnCe/Al_2O_3-PEG.

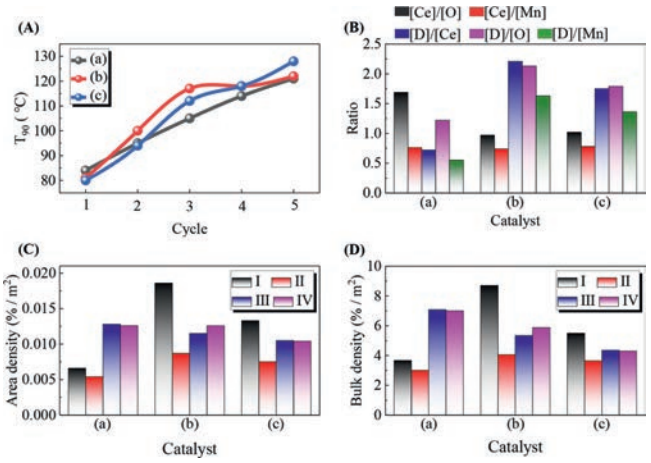

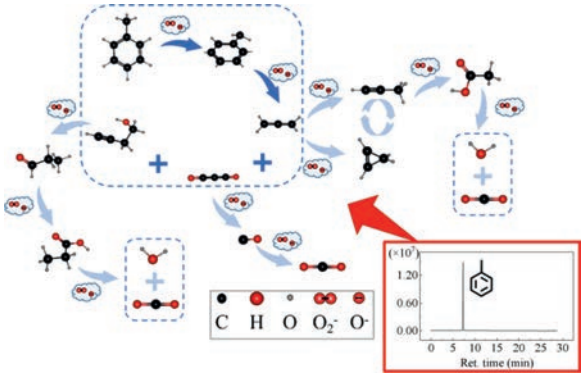

Scheme. 1. The pathway of catalyst.

Fig. 3. (A) T_{90} for evaluation of catalyst activity. (B) Comprehensive analysis of catalyst characterization. (C) Oxygen vacancy surface density and active oxygen species surface density of catalysts. (D) Oxygen vacancy volume density and active oxygen species volume density of catalysts. (a) MnCe/Al_2O_3; (b) MnCe/Al_2O_3-CA; (c) MnCe/Al_2O_3-PEG. [Ce] means $Ce^{3+}/(Ce^{3+} + Ce^{4+})$; [O] means $O_{Ads}/(O_{Ads} + O_{Latt})$; [Mn] means $(Mn^{2+} + Mn^{3+})/(Mn^{2+} + Mn^{3+} + Mn^{4+})$; [D] means D/$F_{2g}$. (I) means [D/$F_{2g}$]/PV; (II) means [O-XPS]/PV; (I) in (C) represents the area density of [D], (II) in (C) represents the area density of [O], (III) in (C) represents the area density of surface oxygen measured by H_2-TPR, and (IV) in (C) represents the area density of surface oxygen measured by O_2-TPD; (I) in (D) represents the volume density of [D], (II) in (D) represents the volume density of [O], (III) in (D) represents the volume density of surface oxygen measured by H_2-TPR, and (IV) in (D) represents the volume density of surface oxygen measured by O_2-TPD.

gen and sub-surface molecule adsorbed oxygen of the three catalysts are basically the same. In this study, the proportions of surface oxygen (SO) and molecular oxygen (O_α), sub surface oxygen (SSO) and atomic oxygen (O_β) are almost equal. The results show that one of the main reasons for the performance difference of the three catalysts is the difference in the relative concentration of surface molecule adsorbed oxygen and sub-surface atom adsorbed oxygen. Comparing the same oxygen species of the three catalysts, it is found that the relative contents of surface oxygen and molecular adsorbed oxygen of MnCe/Al_2O_3-CA are higher than those of other catalysts. It shows that surface molecules adsorb oxygen (SO-O_α) play a major role.

In most studies on catalytic oxidation of toluene, the general conclusion is that toluene is firstly oxidized to benzyl alcohol, then to benzaldehyde and benzoic acid, and finally to water, carbon dioxide and other reaction by-products [49–51]. However, the specific pathway is not clear. In order to further explore the pathway of catalytic ozonation of toluene, *quasi in-situ* GC–MS (Fig. S9 in Supporrting information) was carried out, combined with Raman and FFTIR (Figs. 1B and C) comprehensive analysis. We can find that the main substance detected in the reaction process is toluene, and the content of other substances is very little. According to the CAS numbers and substances corresponding to various peaks, and combined with the relevant theories of chemical reaction, the specific catalytic ozonation pathway of toluene is deduced, as shown in Scheme 1.

The active oxygen species produced by ozone oxidation firstly oxidizes toluene to benzyl alcohol, and then benzyl alcohol is oxidized to allene, carbon suboxide and 3-butyne-1-ol. Among them, (1) Allene is oxidized to cyclopropene and propyne, and cyclopropene can be self converted to propyne. Propyne is oxidized to acetic acid and carbon dioxide, and acetic acid is oxidized to carbon dioxide and water. (2) Carbon suboxide is oxidized to carbon monoxide and carbon dioxide successively. (3) 3-Butyne-1-ol was oxidized successively to propionaldehyde, propionic acid, and finally to carbon dioxide and water. In this study, the reaction pathway runs through the whole reaction system.

Oxygen vacancies and reactive oxygen species are important participants in catalytic oxidation. Reasonable control of the relative content of oxygen vacancies and active oxygen species can effectively improve the performance of the catalyst. In order to explore the relationship between oxygen vacancy and active oxygen species, and the pathway of toluene decomposition in the process of catalytic ozonation of toluene, this study used citric acid and polyethylene glycol as modifiers to prepare the catalyst under the condition of magnetic field.

Combined with the characterization and three properties evaluation of the catalyst, it was found that citric acid could enhance the synergistic effect between Mn and Ce in the catalytic ozonation of

low concentration toluene at low temperature. The closer the concentration ratio of oxygen vacancy formed by Ce to the surface active oxygen species is to 1, and the closer the concentration ratio of oxygen vacancy formed by the synergistic action of Mn and Ce to the surface active oxygen species is to 2, the better the three properties of catalyst are. In addition, higher surface molecule adsorbed oxygen is beneficial to the improvement of the three properties of the catalyst. Finally, the main decomposition pathway of toluene was proposed, which runs through the whole reaction system.

This study provides an important theoretical basis for the catalytic ozonation of VOCs at low temperature, and has a certain reference significance for the application and development in this field. It will be deepened on this basis in the future, such as exploring the influence of water vapor on catalytic ozonation, so as to make the research more practical.

Declaration of competing interest

The authors declear that they have no known competing financial interests or personal relationships that could have appeared to influence the work reported in this paper.

Acknowledgments

This work was financially supported by the Scientific Research Project of Guangzhou City (No. 201804020026), the National Natural Science Foundation of China (Nos. 51878293, 21777047), the National Key Research and Development Program of China (No. 2018YFB0605200), and the Natural Science Foundation of Guangdong Province (No. 2017B090901049).

Supplementary materials

Supplementary material associated with this article can be found, in the online version, at doi:10.1016/j.cclet.2021.09.006.

References

[1] S. Liu, Front. Archit. Civ. Eng. China 3 (2020) 83–86.
[2] Y. Wang, T. Wang, W. Jiang, CEPI 12 (2020) 33–35.
[3] L. Chen, Eng. Min. J. 35 (2019) 255–257.
[4] J. Hao, J. Lan, X. Meng, Y. Fu, Y. Wu, Guangzhou Chem. Ind. 48 (2004) 131–134.
[5] H. Einaga, S. Futamura, J. Catal. 227 (2004) 304–312.
[6] Y. Zhao, H. An, G. Dong, J. Feng, Y. Ren, et al., Appl. Surf. Sci. 505 (2020) 144476.
[7] E. Rezaei, J. Soltan, N. Chen, React. Kinet. Catal. Lett. 136-137 (2013) 239–247.
[8] L. Chen, C. Yang, Special Petrochem. 38 (2021) 69–74.
[9] H. Tian, S. Ni, Q. Yu, H. Li, Y. Liu, Ref. Chem. Ind. 32 (2021) 1–5.
[10] H. Einaga, J. Soltan, J. Catal. 227 (2004) 304–312.
[11] H. Einaga, S. Futamura, React. Kinet. Catal. Lett. 81 (2004) 121–128.
[12] B. Dhandapani, S.T. Oyama, Appl. Catal. B: Environ. 11 (1997) 129–166.
[13] K. Snigdha, S.M. Kumar, S. Pragya, Environ. Technol. 2019 (2019) 1–8.
[14] X. Li, J. Ma, H. He, J. Environ. Sci. 94 (2020) 14–31.
[15] W. Tang, H. Liu, X. Wu, Y. Chen, Ozone-Sci. Eng. 36 (2014) 502–512.
[16] J. Xu, Y. Li, M. Qian, J. Pan, J. Ding, et al., Appl. Catal. B: Environ. 256 (2019) 117797.
[17] H. Huang, J. Lan, J. Wen, Y. Xu, X. Ye, et al., Catal. Today 258 (2015) 627–633.
[18] R. Radhakrishnan, S.Ted Oyama, J. Catal. 199 (2001) 282–290.
[19] E. Rezaei, J. Soltan, N. Chen, J. Lin, Chem. Eng. J. 214 (2013) 219–228.
[20] F. Lin, Z. Wang, Z. Zhang, Y. He, Y. Zhu, et al., Chem. Eng. J. 382 (2020) 123030.
[21] Q. Sun, H. Li, H. Yan, X. Honn, K.S. Hui, et al., Chem. Eng. J. 242 (2014) 348–356.
[22] R. Fang, H. Huang, W. Huang, J. Ji, Q. Feng, Appl. Surf. Sci. 420 (2017) 905–910.
[23] J. Wang, M. Mao, X. Shi, H. Li, H. Huang, et al., J. Environ. Sci. China 40 (2020) 1629–1639.
[24] F. Wang, H. Dai, J. Deng, G. Bai, K. Ji, et al., Environ. Sci. Technol. 46 (2012) 4034–4041.
[25] W. Wang, Q. Meng, Y. Xue, X. Weng, P. Sun, et al., J. Catal. 366 (2018) 213–222.
[26] L. Li, F. Chen, J. Lu, M. Luo, J. Phys. Chem. A 115 (2011) 7972–7977.
[27] X. Lin, S. Li, H. He, Z. Wu, J. Wu, et al., Appl. Catal. B: Environ. 223 (2018) 91–102.
[28] Y. Yuan, Z. Qin, Z. Xu, J. Pan, J. Ding, et al., Catal. Lett. 150 (2020) 365–374.
[29] B. Shen, Y. Yao, H. Ma, T. Liu, Chin. J. Catal. 32 (2011) 1803–1811.
[30] X. Zhang, Y. Liu, J. Deng, X. Yu, Z. Han, et al., Appl. Catal. B: Environ. 257 (2019) 117879.
[31] Z. Lian, J. Ma, H. He, Catal. Commun. 59 (2015) 156–160.
[32] L. Li, G. Hu, J. Lu, M. Luo, Acta Phys. Chim. Sin. 28 (2012) 1012–1020.
[33] J. Jia, P. Zhang, L. Chen, Appl. Catal. B: Environ. 189 (2016) 210–218.
[34] J. Sun, C. Ge, L. An, Q. Tong, F. Gao, et al., J. Chem. Ind. Eng. 71 (2020) 3403–3415.
[35] J.E. Post, D.A. McKeown, P.J. Heaney, Am. Mineral. 105 (2020) 1175–1190.
[36] Y. Zheng, W. Wang, D. Jiang, Chem. Eng. J. 284 (2015) 21–27.
[37] S. Zhao, F. Hu, J. Li, ACS Catal. 6 (2016) 3433–3441.
[38] J. Deng, Y. Zhou, Y. Cui, L. Lan, J. Wang, et al., J. Mater. Sci. 52 (2017) 5242–5255.
[39] N. Huang, Z. Qu, C. Dong, D. Qin, X. Duan, Appl. Catal. A: Gen. 560 (2018) 195–205.
[40] Y. Lee, J. He, A.J. Akey, R. Si, M. Flytzani-Stephanopoulos, et al., J. Am. Chem. Soc. 133 (2011) 12952–12955.
[41] F. Lin, X. Wu, S. Liu, D. Weng, Y. Huang, Chem. Eng. J. 226 (2013) 105–112.
[42] F. Hu, J. Chen, S. Zhao, K. Li, W. Si, Appl. Catal. A: Gen. 540 (2017) 57–67.
[43] Y. Wang, K. Ren, B. Shen, X. Zhang, J. Yang, Chem. Eng. 39 (2020) 3102–3109.
[44] Z. Wang, J. Shen, J. Li, H. Liu, Q. Wang, et al., Appl. Catal. B: Environ. 138-139 (2013) 253–259.
[45] J. Shao, F. Lin, Z. Wang, P. Liu, H. Tang, et al., Appl. Catal. B: Environ. 266 (2020) 118662.
[46] M. Cui, Y. Li, X. Wang, J. Wang, M. Shen, J. Rare Earth 31 (2013) 572–576.
[47] J. Jia, P. Zhang, L. Chen, Appl. Catal. B: Environ. 189 (2016) 210–218.
[48] G. Zhu, J. Zhu, W. Jiang, Z. Zhang, J. Wang, et al., Appl. Catal. B: Environ. 209 (2017) 729–737.
[49] Z. Bo, H. Hao, J. Zhu, J. Yan, K. Cen, Appl. Surf. Sci. 436 (2018) 570–578.
[50] Y. Yang, W. Zhang, J. Wu, M. Fu, L. Chen, et al., J. Environ. Sci. China 33 (2013) 3138–3145.
[51] L. Long, J. Zhao, L. Yang, M. Fu, J. Wu, et al., Chin. J. Catal. 32 (2011) 904–916.